Physicochem. Probl. Miner. Process., 59(6), 2023, 176510

http://www.journalssystem.com/ppmp

Physicochemical Problems of Mineral Processing

ISSN 1643-1049

Synergistic mechanism of dodecylamine/octanol mixtures enhancing lepidolite flotation from the self-aggregation behaviors at the air/liquid interface

Yang Bai [1], Mengxu Xu [1], Weixiang Wen [1], Shifei Zhu [2,3], Weichen Mo [4], Pingke Yan [1]

[1] School of Resources and Environment, Shandong University of Technology, Zibo 255000, China

[2] Jiangsu Design Institute of Geology for Mineral Resources, Xuzhou, Jiangsu 22100, China

[3] CNACG Key Laboratory of Mineral Resource in Coal Measures, Xuzhou, Jiangsu, 221006, China

[4] Changsha Research Institute of Mining and Metallurgy Co., Ltd, Changsha 410012, China

Corresponding author: pingkeyan@126.com (Pingke Yan)

Abstract: Surface tension measurements and molecular dynamics (MD) simulations were used to explore the flotation foam properties and self-aggregation behaviors of dodecylamine (DDA)/octanol (OCT) mixtures formed with different mole ratios at the air/liquid interface. Based on the surface and thermodynamic parameters, the DDA/OCT mixtures exhibited greater interfacial activities and adsorption capacities than their individual components. The MD simulations showed that DDA and OCT were aggregated through hydrogen bonding, coulombic forces and hydrophobic association. OCT was inserted into the DDA adsorption layer, causing the alkyl chains of both DDA and OCT to extend from water to air at varying heights and angles. The addition of OCT improved the hydration of the amino groups and reduced the overall number of hydrogen bonds. The stability of the flotation foam decreased, and the high viscosity and difficult defoaming of the DDA flotation foam were significantly improved. When the DDA/OCT mole ratio was 2:1, the included angle formed between the alkyl chains and the interface was maximized, leading to enhanced compatibility among the alkyl chains, and the hydrogen bond energy was relatively large, which showed a strong synergistic effect. The MD simulation findings were consistent with the results obtained from the lepidolite flotation and surface tension experiments conducted in this study; our results could provide a theoretical foundation for the selection of superior mixed collectors and frothers.

Keywords: DDA/OCT mixtures, self-aggregation behaviors, flotation foam, molecular dynamics simulations, surface tension, air/liquid interface

1. Introduction

Lithium, as the most indispensable energy storage metal, has reached a strategic level and become the real white oil in the background of global carbon neutrality. The world is rich in lithium resources, and salt lake brine and spodumene account for over 70% of the total resource reserves (Meng et al., 2021; Pankaj et al., 2016). However, with breakthrough lithium extraction technology and production process progress, lepidolite has become another important lithium source, and its strategic value is increasing yearly. Lepidolite is usually associated with chlorite, kaolinite, albite and other clay minerals, and with the depletion of the flak lepidolite resources, fine-grained inlaid lepidolite has become another important source of lepidolite at this stage; thus, flotation is usually used for enrichment (Zhiqiang et al., 2021).

Flotation is an efficient method for separating ores by using the differences in physicochemical properties of the mineral surfaces, and it is extensively used in mineral processing. Lepidolite is a typical two-layer-structured phyllosilicate, and the lithium ions between layers are easily dissolved in the pulp to provide a negatively charged mineral surface over a wide pH range. Therefore, conventional lepidolite flotation is performed by using cationic surfactants (mainly amine surfactants) as collectors under acidic conditions; this method has been shown to be reliable and applicable to industrial

DOI: 10.37190/ppmp/176510

production (Sekulić et al., 2004; Pugh et al., 1996). However, this approach still has some drawbacks: first, the amine surfactants need to be heated at low temperatures to ensure dispersibility; second, strongly acidic solutions corrode the flotation equipment and potentially impact the environment; and third, the existence of slime causes a large amount of foam produced by a single amine surfactant, which damages the flotation environment (Yang et al., 2022).

To maximize the synergism of mixed surfactants in flotation, alcohols are often incorporated into the formulations of the mixed surfactants (Nishikido, 1977). Mixed amine/alcohol surfactants retain the advantages of the amine surfactants, such as simple reagent systems, minor metal ion influences and preferable adaptability; additionally, they overcome the shortcomings of single amine surfactants and have attracted extensive attention in nonmetallic mineral flotation (Li et al., 2015). Jiang et al. investigated muscovite flotation in the presence of cetyltrimethylammonium chloride/octanol (OCT) mixtures. The mixtures exhibited greater interfacial activities and better collecting abilities than their components (Hao et al., 2017). Zhang et al. found that dodecylamine (DDA)/monohydric alcohol mixtures provided better flotation performance than their components during dolomite flotation. The combination of DDA and alcohol resulted in more extensive adsorption of alcohol on the mineral surface, and the mixtures exhibited more efficient collection than DDA alone (Han et al., 2019). Many studies have investigated the synergism of mixed amine/alcohol surfactants in mineral flotation; however, most were focused on the solid/liquid interface. As the dominant collectors, amine surfactants initially undergo selective adsorption on the target mineral surface. The alcohols, as the auxiliary collectors, are indirectly adsorbed on the mineral surface, and a synergistic effect with the amine surfactant enables co-adsorption. The mixed surfactant forms a more uniform adsorption layer on the mineral surface than the single surfactants and is more likely to exhibit hemimicelle adsorption (Bahareh et al., 2014; Vidyadhar et al., 2012). However, in-depth research has shown that the self-aggregation behaviors of amine/alcohol mixtures at the air/liquid interface are equally crucial. Because of their excellent foaming properties, amine surfactants and alcohols are also used as frothers during flotation. Therefore, the amine/alcohol mixtures affect the properties of the flotation foam, further affecting the flotation experimental indicators. Numerous studies have indicated that the strong synergistic effects between the amine surfactants and alcohols change the surface tension. Alterations in the hydrodynamic characteristics and foam properties, such as those resulting in the formation and stability of foams, can have an impact on foam mineralization and the collection of target minerals during flotation (Li et al., 2017; Szymczyk et al., 2007). Therefore, the performance of the amine surfactants and alcohols at the air/liquid interface needs to be investigated.

The purpose of this investigation is to elucidate the synergy of the amine/alcohol mixture in lepidolite flotation from the perspective of the air/liquid interface. In this paper, DDA, a representative amine surfactant, was mixed with different mole ratios of OCT. Surface tension measurements, foam performance experiments and molecular dynamics (MD) simulations were used to explore the interfacial properties and self-aggregation behaviors of DDA/OCT mixtures at the air/liquid interfaces (Jesús et al., 2019; Simon et al., 2020; Stefan et al., 2016); the results could provide a theoretical foundation for the selection of superior mixed collectors and frothers.

2. Experimental

2.1. Mineral and reagents

The lepidolite ore used for flotation experiments was purchased from Jiangxi Province, China. The specimens were manually picked and ground to -0.074 mm accounting for 80% by a ceramic ball mill. Based on X-ray fluorescence spectrometer method, the chemical composition of the samples included 1.09% Li_2O, 67.95% SiO_2, 17.37% Al_2O_3, 1.63% Na_2O, 3.12% K_2O, 0.55% Fe_2O_3, 0.28% MgO, 3.04% CaO and 3.34% others. All reagents, including DDA, OCT, NaOH and hydrochloric acid, were analytically pure and purchased from Shantou Xilong Scientific Co., Ltd., China. Doubly distilled water was used in flotation experiments and performance tests.

2.2. Flotation experiments

Flotation experiments were carried out with a flotation cell containing 125 g of the lepidolite samples and 500 mL of doubly distilled water. The flotation cell was suspended on a laboratory XFD flotation

machine (XFD, Jilin Exploration Machinery Corp., Changchun, China) operating at 1800 r/min with an aeration amount of 0.1 $m^3/(m^2 \cdot min)$. The pH of the suspension was adjusted with hydrochloric acid and NaOH after mixing for 1 min. Then, DDA and OCT were sequentially added, and the pulp was conditioned for 1 min for each surfactant addition, followed by a flotation collection period of 3 min; the total dosage of the mixed surfactant was 5.0×10^{-4} mol/L. The froth products and tailings were weighed, dried and weighed again to calculate the flotation recovery. The temperature of the flotation was maintained at 20 ℃, and the final value was reported as the average result from three tests for each sample.

2.3. Surface tension measurements

Surface tension measurements were carried out to assess the interfacial activity of the pure surfactants and the DDA/OCT mixtures. The Wilhelm platinum ring detachment method was utilized for measuring the surface tensions at 20 ℃ with a K100 tensiometer from Krüss, Inc., in Germany. Before each measurement, the platinum ring was rinsed and heated with an alcohol blowlamp flame to remove residue from the previous measurement, and each sample was stabilized for 10 min in the instrument to equilibrate the surface tension. The surface tension was measured five times to ensure the precision of the result, and the final value was the average of the duplicate measurements.

2.4. Foam performance experiments

The effects of DDA/OCT mixtures with different mole ratios on the flotation foam properties were examined with the air filling method. Foaming capacity and foam stability are usually characterized by the height, half-life, and moisture content of the foam layer. The specific experimental procedures were performed as follows: (1) Based on the flotation experimental conditions, the ore sample, deionized water, surfactants and pH modifiers were fully mixed in the flotation cell, as shown in Fig. 1. (2) The feed valve of the connected vessels was opened, and 100 mL suspension flowed into the measuring cylinder. (3) The inlet valve was opened at the bottom of the measuring cylinder. The suspension was inflated for 10 seconds at an aeration volume of 0.1 $m^3/(m^2 \cdot min)$, and then the maximum foam layer height and the half-life were recorded. (4) The floated products were collected and then weighed. (5) The concentrated products were dried at 105 ℃ and weighed to calculate the moisture content of the foam.

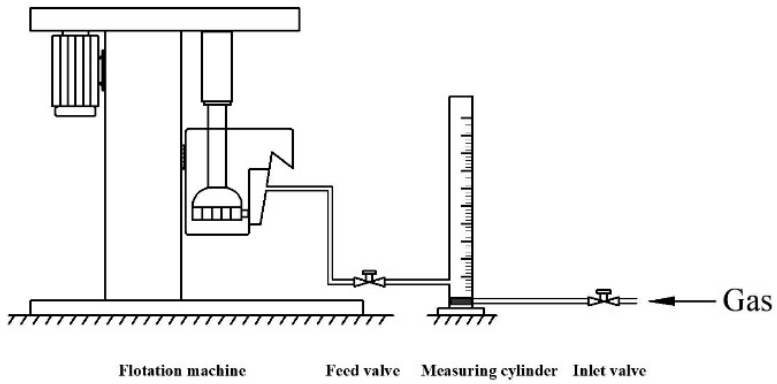

Fig. 1. Schematic diagram of the foam performance experiments

2.5. MD Simulations

2.5.1. Surfactant molecular model

DDA is mainly present in an ionic state in neutral solutions, and OCT does not become ionized in aqueous solutions. Therefore, the surfactant models for the DDA cations and OCT molecules were constructed for the MD simulation. The surfactant model was established by the Visualizer module in Material Studio software, and the partial charge distributions of the surfactant molecules were determined with density functional theory; which was conducted with the DMol^3 module of Materials Studio software using the GGA/PBE method. Additionally, the entire simulation system was subjected

to water solvation. The accuracy of the surfactant model was ensured by controlling the convergence accuracy during the calculation process. In which, maximum inter-atomic force 0.001 Ha/Å, real space cutoff radius 4.5 Å, and maximum displacement 0.005 Å, convergence energy tolerance 1.0×10^{-5} Ha. Finally, frequency analyses were conducted on the optimized models to confirm the minimum energy. The atomic structures and electron distributions of the two surfactants are shown in Fig. 2.

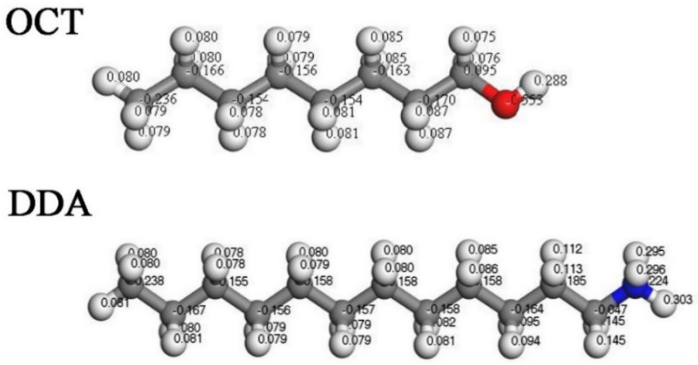

Fig. 2. Atomic structures and partial charge distributions of the surfactant molecules (The hydrogen, chlorine, carbon, nitrogen and oxygen atoms are white, green, gray, blue and red, respectively; the same below)

The simulation models, including the total numbers of DDA cations, OCT molecules, chloride ions, and water molecules, were constructed in the Amorphous Cell module of Materials Studio software under periodic boundary conditions. The initial configurations were constructed in the following order: (1) Based on the relevant literature and our simulation results (Li et al., 2016), the surface areas of DDA and OCT at the air/water interface were 75-88 $Å^2$ and 62-81 $Å^2$, respectively. For convenience in subsequent simulations, the mean surface areas of these two surfactants were set to 80 $Å^2$. (2) A water slab with dimensions of 49×49×38 Å along the x-, y-, and z-directions was filled with 3000 water molecules. To prevent periodic replication, two vacuum slabs with thicknesses of 60 Å were positioned on the upper and lower sides of the water slab along the z direction to form the air/liquid interface. (3) Two monolayers containing a total of 60 surfactant molecules were placed on opposite sides of the water slab, with their head groups in the water slab and alkyl chains in the vacuum slab; each monolayer consisted of the same number of DDA cations and OCT molecules. (4) Chloride ions were introduced as counterions to maintain the overall electrical neutrality of the simulation system. (5) A simulated initial structure was established for the DDA/OCT mixture monolayer at the air/liquid interface. The substance compositions in various simulation systems are shown in Table 1.

Table 1. The substance compositions in various simulation systems.

Mole ratio (DDA:OCT)	Number of molecules or ions			
	DDA cations	OCT molecules	Chloride ions	Water molecules
1:0	60	0	60	3000
3:1	45	15	45	3000
2:1	40	20	40	3000
1:1	30	30	30	3000
1:2	20	40	20	3000
1:3	15	45	15	3000
0:1	0	60	0	3000

2.5.2. MD simulation details

The Forcite module of Materials Studio software was utilized to perform all-atom MD simulations. The self-aggregation process at the air/liquid interface was simulated under the PCFF-INTERFACE forcefield, and the potential energy parameters of the DDA cations, OCT molecules, chloride ions and

water molecules were determined with this forcefield. This forcefield could accurately simulate the interfacial behavior, and numerous related studies have confirmed that the forcefield effectively performs during the self-aggregation process of the mixed surfactants at the air/water interface (Hendrik et al., 2013; Lin et al., 2016; Qinhong et al., 2018). During the simulations, geometry optimization was initially utilized to minimize the initial energy of the simulation system with over 50,000 steps. Then, the NVT assembly was used for the simulation calculations, and the Hoover-Nosé thermostat was employed to maintain a constant temperature of 293 K. A Maxwell–Boltzmann distribution was used to randomly assign an initial velocity to each molecule, and the Velocity Verlet algorithm was utilized to solve the Newtonian motion equation. The Ewald summation method was used to explain the long-distance correction of the electrostatic and van der Waals interactions with a cutoff of 12.5 Å. The total running time of the MD simulation was 10 ns with a time step of 1 fs, and the final 1 ns was used for the statistical analyses.

3. Results and discussion

3.1. Flotation results

Studies have shown that the addition of alcohols to amine surfactants enhanced the lepidolite collection efficiency and significantly improved the adaptability of the amine surfactants to the pulp pH during flotation (Nathália et al., 2016; Yang et al., 2023). Fig. 3 shows the results for lepidolite flotation with different surfactants at a pH of 6. The collecting ability and selectivity of DDA for lepidolite were worse than those of the DDA/OCT mixtures in a neutral environment, indicating a positive synergy between DDA and OCT. As an auxiliary surfactant, OCT was not ionized in the aqueous solution; thus, it could not collect lepidolite, and the flotation recovery was close to 0. However, due to the fine particle sizes of the raw ore, some lepidolite with gangue was scraped out due to the natural hydrophobicity of the lepidolite surface and the strong foaming ability of OCT. Therefore, the Li_2O grade of the flotation concentrate was slightly higher than that of the raw ore. The DDA/OCT mixtures with different mole ratios exhibited different lepidolite flotation capabilities. As the OCT mole ratio increased, the recovery and grade of the resulting Li_2O initially increased and then decreased. The flotation performance was worse than that of pure DDA at a DDA/OCT mole ratio of 1:3, showing that the addition of OCT to the DDA within a certain range improved the lepidolite flotation performance; however, excessive OCT addition led to deterioration. These flotation results were consistent with Wang's research findings (Li et al., 2015).

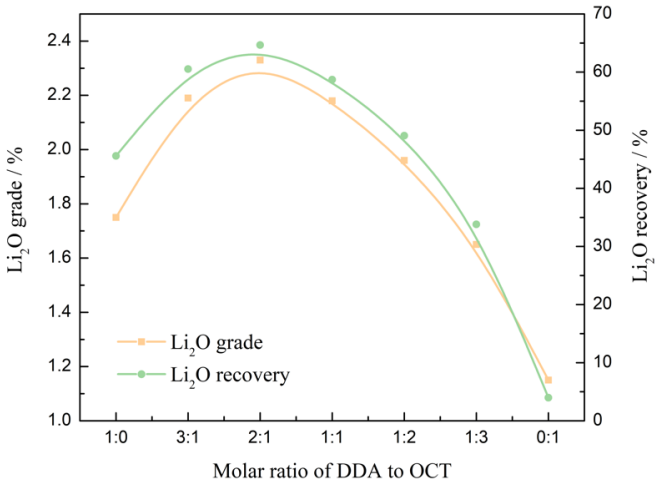

Fig. 3. Lepidolite flotation results with different DDA/OCT mole ratios at a pH of 6

3.2. Foam properties

The synergy between the alcohol and amine surfactants during flotation of mica minerals was confirmed in numerous studies; however, most results were limited to the solid/liquid interface. As a broad-spectrum silicate collector, DDA also served as a frother in the lepidolite flotation, and the high

viscosity foam seriously affected the concentrate grade. Hence, additional research was needed to determine the effects of the foam properties with the DDA/OCT mixtures.

Table 2 lists the foam properties of DDA/OCT mixtures formed with different mole ratios. Relative to the DDA/OCT mixtures, the use of only DDA yielded the maximum height, half-life, and water content in the foam layer, providing evidence that the DDA flotation foam exhibited superior foaming power and higher stability. Since the foaming ability of DDA was better than that of OCT, the foaming ability of the DDA/OCT mixtures weakened with increased OCT amounts; this was observed by the decreased foam layer height. The excess stability of the DDA flotation foam was also significantly improved after adding the OCT, and the half-life and water content of the flotation foam significantly decreased with increases in the OCT amount. Flotation can be negatively impacted by various factors, such as gangue entrainment and slime cover, which are often caused by foams with high viscosity and excess stability. However, foams with low stability can potentially break during flotation, leading to desorption of the target mineral (Gupta et al., 2007; Laskowski et al., 2003). Upon comparing the experimental results described in section 3.1, a correlation was observed between the reduced stability of the DDA flotation foam within a certain range and the improved flotation performance. Additionally, the optimal DDA/OCT mole ratio was determined to be 2:1.

Table 2. Foam properties of DDA/OCT mixtures formed with different mole ratios.

Mole ratio (DDA:OCT)	Foam layer		
	Height/mm	Half-life/s	Moisture content/%
1:0	62	267	74.52
3:1	54	165	66.02
2:1	49	152	64.14
1:1	46	143	62.52
1:2	43	136	60.93
1:3	42	131	57.68
0:1	40	127	53.69

3.3. Surface tension

Generally, a lower surface tension in a mixed amine/alcohol surfactant correlates to a stronger synergistic effect, resulting in improved flotation performance (Yang et al., 2021). The surface tension rapidly decreased as the surfactant concentration was increased, and it remained constant upon reaching saturation for the surfactant adsorbed at the air/liquid interface (Fig. 4). The DDA/OCT mixtures had lower surface tensions and critical micelle concentrations (CMCs) than the pure DDA; this result supported the hypothesis that a surface-active complex formed and was adsorbed at the solution surface. Due to the ion–dipole interactions of the head groups, the insertion of OCT into the DDA adsorption layer reduced the electrostatic repulsions among the DDA cations and increased the amount of DDA/OCT mixture adsorbed at the air/liquid interface (Lucassen-reynders et al., 1981). Moreover, the reduced CMCs indicated that hemimicelle adsorption more easily occurred on the solid/liquid interface, and the OCT partially replaced the DDA during flotation; this reduced the amount of DDA needed and the production costs(Monte et al., 2004; Hao et al., 2019). Clearly, the mole ratios in the DDA/OCT mixtures affected the surface tensions and CMCs. As the mole proportion of OCT was increased, the surface tension and the CMC initially increased and then decreased; the minimum value was reached at a DDA/OCT mole ratio of 2:1; this result agreed with the observations from the flotation experiments.

The different surface and micelle formation parameters for the DDA/OCT mixtures were calculated with equations (1) – (3), and the relevant parameters are provided in Table 3.

$$\Gamma_{max} = -\frac{1}{2.303nRT}\left(\frac{\partial\gamma}{\partial \log C}\right)_T \tag{1}$$

$$A_{min} = \frac{10^{18}}{\Gamma_{max} N_A} \tag{2}$$

$$\Delta G_m^0 = RT \ln X_{cmc} \quad (3)$$

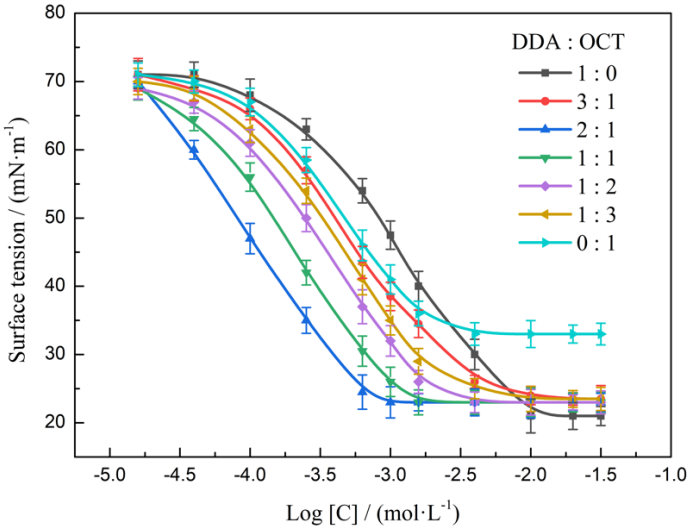

Fig. 4. Surface tensions of the DDA/OCT mixtures and their components at different concentrations

where $(\partial\gamma/\partial \log C)_T$ is the slope of the linear portion of a plot of surface tension vs. log surfactant concentration at 293 K, the value of 2.303 is approximately equal to value of ln(10), R is the universal gas constant (8.314 J·mol^{-1}·K^{-1}), T is the absolute temperature (293 K), n is the number of ionic species (n = 1 for mixed surfactant system, n = 2 for pure surfactant system), N_A is the Avogadro constant (6.02×10^{23} mol^{-1}), X_{cmc} is the CMC at the given mole proportion (mol·L^{-1}), Γ_{max} is mol·m^{-2}, A_{min} is nm^2, and ΔG_m^0 is kJ·mol^{-1}. Due to the low concentration of surfactant at the air/liquid interface, the activity in the standard Gibbs adsorption equation could be replaced by the concentration. To simplify the calculation, counterion bonding was not considered in the ΔG_m^0 calculation (Wenfeng et al.,2021).

Table 3 Interfacial and thermodynamic properties for DDA/OCT mixtures.

Mole ratio (DDA:OCT)	CMC/(mol·L^{-1})	γ_{CMC}/(mN·m^{-1})	Γ_{max}/(mol·m^{-2})	A_{min}/nm^2	ΔG_m^0/(kJ·mol^{-1})
1:0	1.96×10^{-2}	20.53	1.64×10^{-6}	1.01	-9.58
3:1	1.22×10^{-2}	23.36	3.48×10^{-6}	0.48	-10.74
2:1	1.10×10^{-3}	23.81	5.17×10^{-6}	0.32	-16.60
1:1	2.00×10^{-3}	24.05	4.47×10^{-6}	0.37	-15.15
1:2	5.12×10^{-3}	23.21	3.93×10^{-6}	0.42	-12.86
1:3	8.91×10^{-3}	24.21	3.54×10^{-6}	0.47	-11.51
0:1	4.79×10^{-3}	33.23	1.85×10^{-6}	0.90	-13.02

The Γ_{max} value is the saturation amount of the surfactant adsorbed at the air/liquid interface and used as a basic indicator to assess the adsorption effects of the surfactants. The Γ_{max} values of the DDA/OCT mixtures were greater than that of pure DDA, and Γ_{max} peaked when the DDA/OCT mole ratio was 2:1 (Table 3). A higher Γ_{max} value correlated to a higher adsorption capacity of the surfactants at the air/liquid interface and a denser arrangement. Consequently, the molecular configurations observed in the DDA/OCT mixtures were notably more compact, indicating that the mixed surfactant molecules showed a more vertical configuration at the interface compared to pure DDA. Similarly, the A_{min} value is the average minimum area per molecule adsorbed at the air/liquid interface, and its change was exactly opposite to that of the Γ_{max} value. With a decrease in the DDA mole proportion, the A_{min} values for the DDA/OCT mixtures initially decreased and then increased; this result was attributed to the differences in the ion–dipole interactions between DDA and OCT at different mole ratios (Longhua et al., 2016; Sufen et al., 2010). All of the ΔG_m^0 values were negative, indicating that the

thermodynamic processes of the mixed systems were spontaneous. To determine reason for the optimal synergistic effect for the DDA/OCT mole ratio of 2:1, MD simulations were used to investigate the self-aggregation of the DDA/OCT monolayers at the air/liquid interface.

3.4. Self-aggregation of the DDA/OCT mixtures

Relative to their initial structures, each system displayed a relatively disordered state in the simulations (Fig. 5). The DDA/OCT mixtures formed tightly packed monolayers with their head groups penetrating the water phase and their alkyl chains stretched into the air with various incline angles. The mixed systems exhibited homogeneous distributions and interweaving arrangements of the DDA cations and OCT molecules at the air/liquid interface. Specifically, the head groups were completely miscible with water, showing that they were completely hydrated. Due to the hydrophobic association, penetration of the water molecules into the surfactant monolayer was limited; thus, only a portion of the alkyl chains were hydrated. Coulomb forces caused the chloride ions to disperse around the amino groups, and no water molecules escaped the monolayer during the simulations.

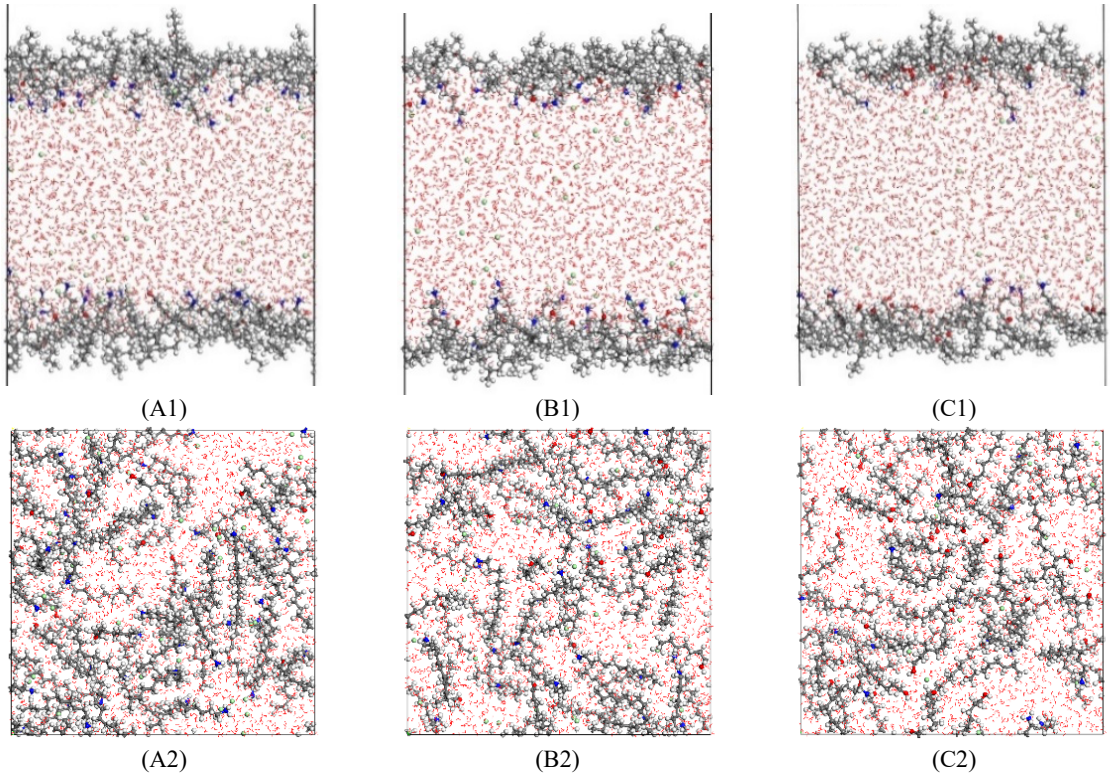

Fig. 5. Final configurations of mixed surfactants with different molar ratios (a) DDA:OCT=3:1; (b) DDA:OCT=1:1 and (c) DDA:OCT=1:3, shown in front view (A1, B1 and C1) and top view (A2, B2 and C2)

To explore the detailed differences in the self-aggregation behaviors of the DDA/OCT mixtures formed with different mole ratios, the relative concentration distributions of the molecules, groups and atoms in the simulation systems were calculated. The coordinate origin for the simulation system was set at the center of the slab, and the results were shown as the average for the simulation slab. From Fig. 6, the peaks of the amino groups and hydroxyl groups in the mixed surfactants were completely in the water phase; additionally, the peak of the hydroxyl groups was closer to the air phase than that of the amino groups, indicating that the amino groups were more hydrophilic. However, regardless of the DDA/OCT mole ratio, the hydroxyl groups were always near the amino groups, showing that there were interactions between them (Li et al., 2017). With increasing OCT amounts, the peak intensity for the chloride ions decreased. Although OCT was not ionized in the aqueous solutions, the high electronegativity of the hydroxyl group weakened the electrostatic attractions between the amino groups and chloride ions, causing the chloride ions to migrate toward the bulk water molecules over time.

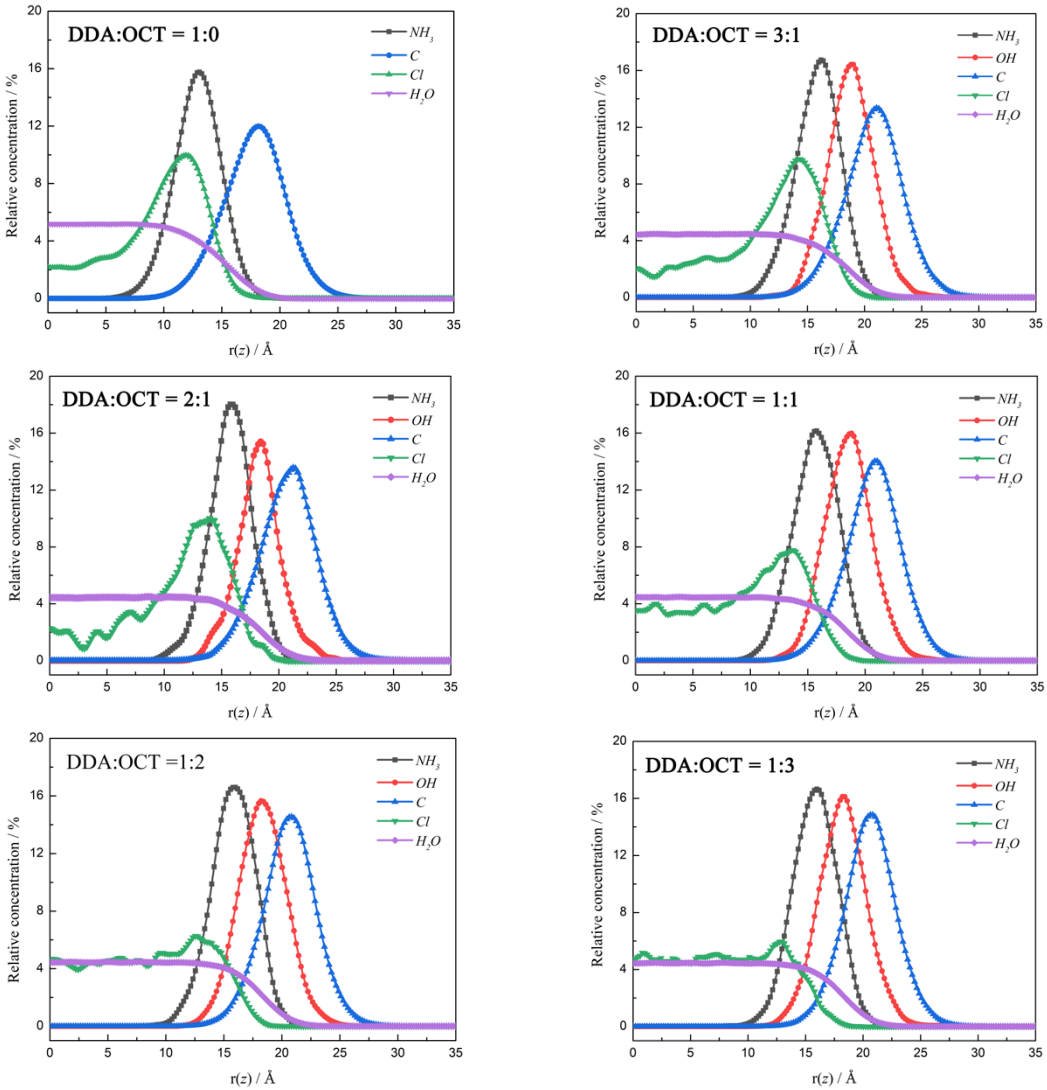

Fig. 6. Relative concentration distributions for the various components along the z direction (NH_3: amino group; OH: hydroxyl group; C: carbon atom; Cl: chloride ion; H_2O: water molecule.)

3.5. Interactions between DDA and OCT

To determine the interactions between DDA and OCT, the radial distribution functions (RDFs) for the nitrogen (N_{amino}) atoms in the amino groups and oxygen ($O_{hydroxyl}$) atoms in the hydroxyl groups were calculated. The peaks for the N_{amino}–N_{amino} atom RDF in the pure DDA system were observed at 3.85 Å and 5.18 Å (Fig. 7(A)). In the mixed systems, the peaks gradually decreased until they disappeared with increasing OCT amounts. When the DDA/OCT mole ratio was less than 3:1, a broad peak for the N_{amino}–N_{amino} atom RDF was observed at approximately 8 Å, indicating that the distance between the amino groups in the pure DDA system was smaller than those for DDA/OCT mixture systems. The abundance of DDA present at the air/liquid interface and the electrostatic repulsions between the amino groups were the main factors contributing to this phenomenon. DDA was uniformly distributed at the air/liquid interface without aggregation in the pure DDA system, and the electrostatic repulsions improved the stability of the DDA flotation foam. With increases in the OCT amount, the DDA was moved by electrostatic repulsions; OCT was inserted into the adsorbed DDA monolayer due to the synergistic effect, which increased the distances between the amino groups. The presence of hydroxyl groups weakened the electrostatic repulsions among the DDA cations, affecting the stability of the flotation foam at the air/liquid interface. The stability of the DDA flotation foam began to decline. When the distances between the amino groups reached 8 Å, relative equilibrium was reached. Based on the RDFs for the H_{amino} atoms (hydrogen atoms in the amino groups) and the $O_{hydroxyl}$ atoms in Fig. 7(B),

two major peaks were observed; one was at 2.02 Å, and the other was at 5.16 Å; this result indicated that hydrogen bonding and electrostatic forces constituted the primary interactions between the amino and hydroxyl groups (Jaewook et al., 2011).

Fig. 8 shows the relative concentration distributions for the carbon atoms in the mixed systems

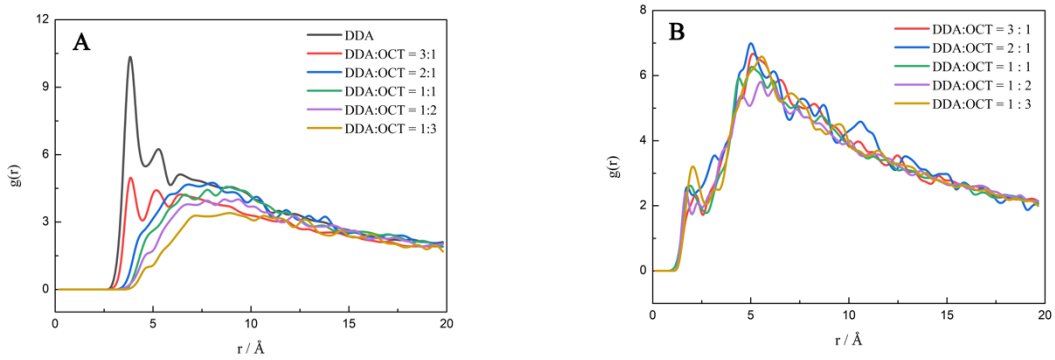

Fig. 7. RDFs for the N_{amino} atoms to N_{amino} atoms (A) and H_{amino} atoms to $O_{hydroxyl}$ atoms (B)

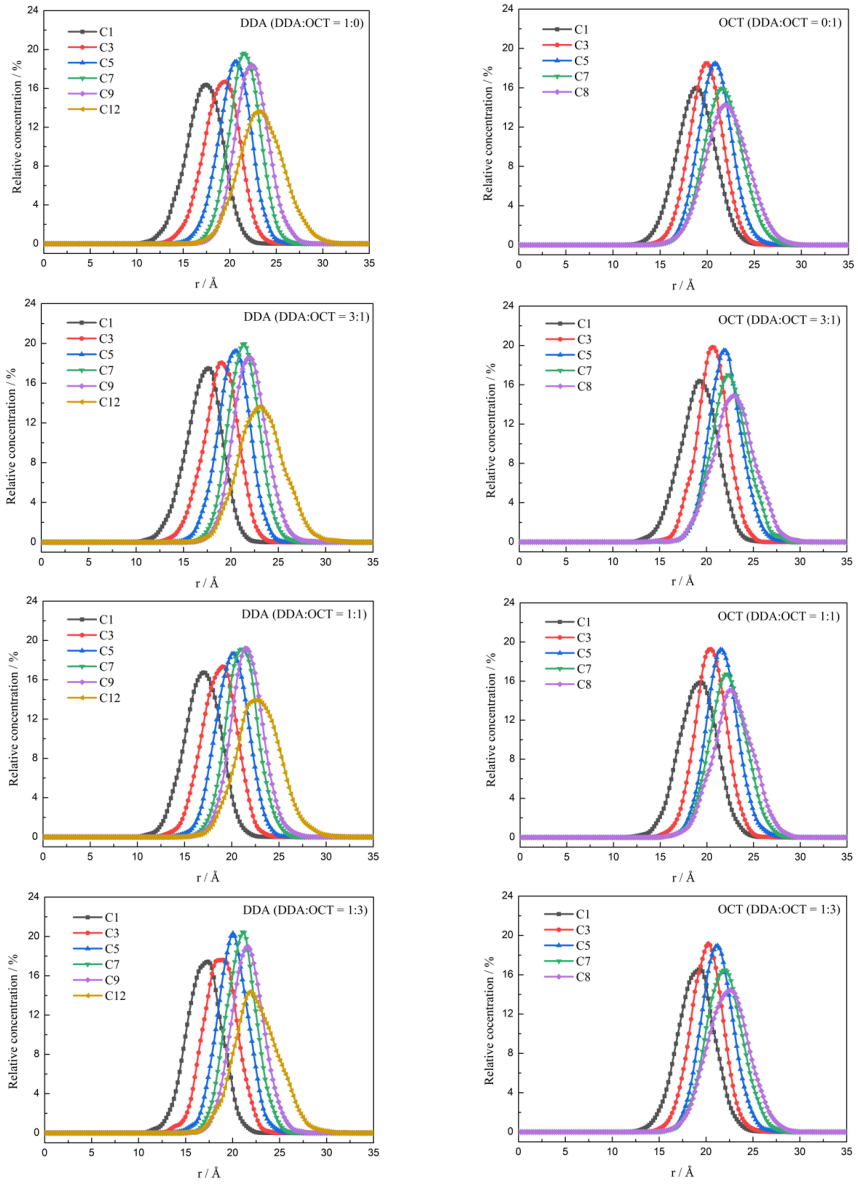

Fig. 8. Relative concentration distributions for the carbon atoms along the z direction (As the distance from the head group increases, the carbon atoms of the alkyl chain are represented as C1, C2, C3, etc.)

along the z direction. The carbon atom distributions for DDA and OCT at the air/liquid interface were different in pure surfactant systems. Specifically, due to the strong hydrophilicity of the amino group, the first carbon atom (C1) of DDA was farther from the interface than the C1 atom of OCT in the water phase. Because of the short carbon chain of OCT, the last carbon atom (C8) was closer to the interface than the last carbon atom (C12) of DDA in air. However, due to the synergism between DDA and OCT, the concentration distributions for the carbon atoms greatly changed. Although the C1 peak positions for DDA and OCT were different, the peak positions for the last carbon atoms were the same, indicating that the alkyl chains in the mixed systems had strong hydrophobic associations, and the strength of this hydrophobic association was closely related to the mole ratio.

Fig. 9 shows the density distributions for the carbon atoms at the air/liquid interface along the x direction. The flat curve indicated a relatively uniform surfactant distribution at the air/liquid interface. The low heterogeneity observed for the pure DDA monolayer at the air/liquid interface indicated a relatively homogeneous distribution of the surfactants. The DDA/OCT monolayers has greater heterogeneity in the mixture systems, and the nonuniformity of the density curve showed an initial increase followed by a decrease with increasing OCT amounts; the maximum value resulted when the DDA/OCT mole ratio was 2:1. We deduced that adding OCT to DDA improved the compatibilities of the alkyl chains and that the DDA/OCT mixtures had more compact arrangements than DDA at the interface. From another perspective, this also indicated that the presence of OCT destroyed the stability of the DDA cations resulting from electrostatic repulsion. The viscosity of the DDA flotation foam decreased, causing an easier defoaming (Ximei et al., 2021). However, the high compatibilities of the alkyl chains resulted in higher concentrations of surfactant molecules absorbed at the air/liquid interface; thus, the downward trend for foam stability over time was slowed. Therefore, the DDA/OCT foam was not easily disrupted during floating.

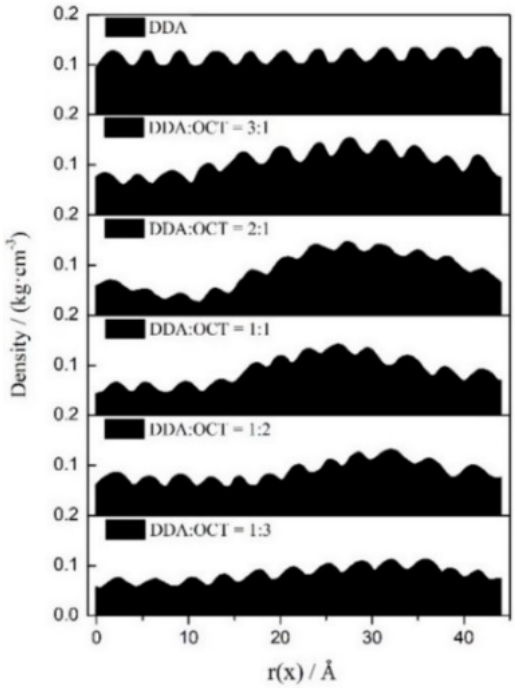

Fig. 9. Density distributions of the carbon atoms in the mixtures at the air/liquid interface along the x direction

Fig. 10 shows the included angles between the alkyl chains of the DDA and the air/liquid interface under different mole ratios. The included angle was closely related to the mole ratio of the mixture. With a decrease in the OCT amount, the included angle initially increased and then decreased, and the maximum included angle was reached when the DDA/OCT mole ratio was 2:1, which was consistent with the flotation experiments. Under this molar ratio, the included angle of the mixed surfactant was greater than that of the pure DDA, indicating that the alkyl chains of the mixed surfactants were more vertically oriented at the air/liquid interface. Therefore, the mixed DDA/OCT surfactants display much greater compactness than pure DDA, facilitating the expression of their hydrophobicity (Li et al., 2016).

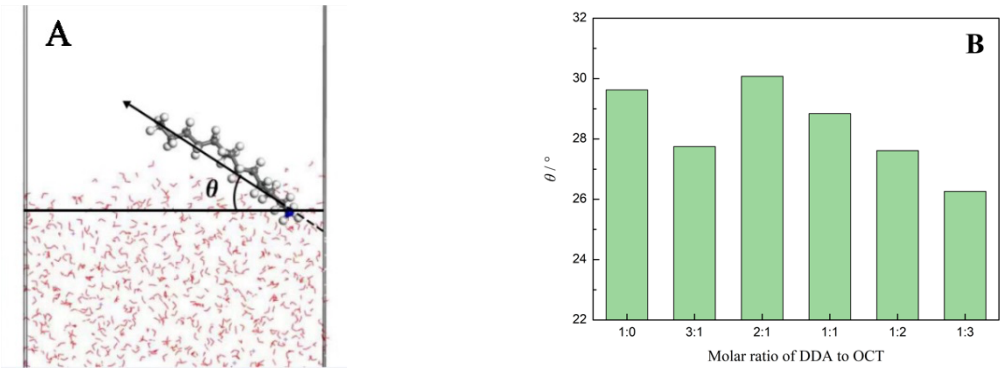

Fig. 10. Comparison diagram for the included angles between the alkyl chains of DDA and the air/liquid interface (A) and evolution of their angles (B)

3.6. Interactions between surfactants and water molecules

The interfacial characteristics of surfactants depend on their interactions with water molecules. To compare the interactions for different simulation systems, the RDFs between the head groups and the water molecules were calculated. The RDFs in Fig. 11(A) show the distances between the H_{amino} atoms and oxygen (O_{water}) atoms in the water molecules. The RDFs for the H_{amino} and O_{water} atoms were similar for the different simulation systems, and the presence of OCT did not modify the two hydration shells encircling the amino groups, as evidenced by the presence of strong peaks at 1.74 Å and 3.16 Å. The first hydration shell originated from hydrogen bonding between the H_{amino} and O_{water} atoms, and the second hydration shell was the network of neighboring hydrogen atoms that interacted with the water molecules in the first hydration shell. Prior research established that the first hydration shell was a critical factor influencing the interactions between the head groups and water molecules (Taotao et al., 2010). In comparing the peaks at 1.74 Å, the peak intensities for the mixture systems surpassed that of the pure DDA system, indicating that adding OCT to DDA improved the hydration of the amino groups. There were two reasons for this. First, the decreased DDA amount caused diffusion of the DDA cations due to the electrostatic repulsion, and the water molecules filled the vacancies left by DDA. Similarly, the high electronegativity of the hydroxyl group reduced the chloride ion concentration surrounding the amino groups, causing the water molecules to fill the holes left by chloride ions. Moreover, the substantial presence of the water molecules surrounding the head groups served to screen the electrostatic repulsions and reduced the overall interaction strengths between the surfactants; this resulted in a loose molecular accumulation of the mixed surfactant molecules at the air/liquid interface.

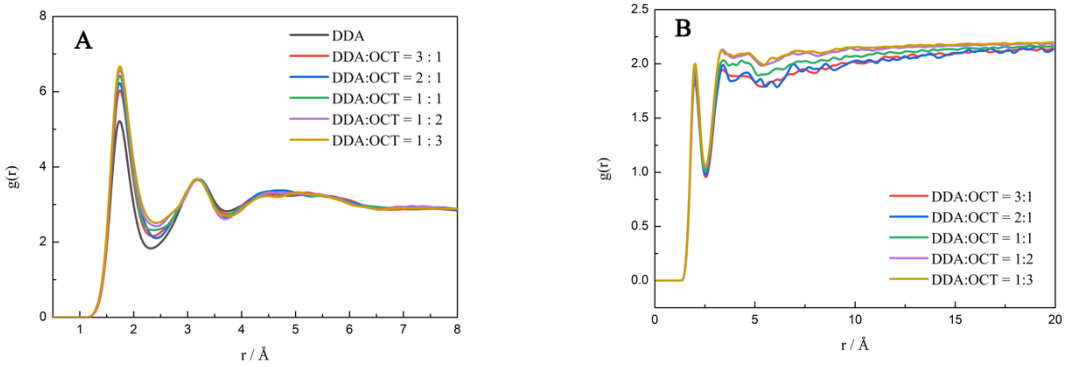

Fig. 11 RDFs for the H_{amino} to O_{water} atoms (A) and $O_{hydroxyl}$ to H_{water} atoms (B) in the different systems.

Fig. 11(B) shows the RDFs for the $O_{hydroxyl}$ to hydrogen (H_{water}) atoms in water molecules. The shapes of the RDF curves were similar for all systems, and a peak was observed at 2.05 Å; this result indicated that the distances between the hydroxyl groups and the water molecules were longer than those between the amino groups and the hydroxyl groups (Fig. 7(B)), and the interactions were hydrogen bonding. The peak intensity strengthened with a decreased amount of DDA; however, the intensity

change was much smaller than that of the H_{amino}–O_{water} atom RDF (Fig. 11(A)). This result was mainly caused by the steric hindrance due to the presence of DDA. An amino group has three hydrogen atoms and occupies more space than a hydroxyl group. With decreases in the DDA amount, the steric hindrance decreased, and the number of water molecules surrounding the hydroxyl groups slightly increased. In comparison, the peak intensity for the H_{amino}–O_{water} atom RDF was stronger than that for the $O_{hydroxyl}$–H_{water} atom RDF. Thus, the interactions between the amino groups and the water molecules were significantly more robust than those between the hydroxyl groups and the water molecules (Li et al., 2017). Interestingly, the interactions between the amino and hydroxyl groups, amino groups and water molecules, hydroxyl groups and water molecules, as well as water molecules themselves were dominated by hydrogen bonding; the comprehensive effects of these four interactions impacted the flotation foam properties. Table 4 shows the bond angles and bond lengths for the hydrogen bonds arising from different sources. In pure water systems, the bond lengths and bond angles were 1.97 Å and 152.68°, respectively; these values were the same as those calculated in other studies (Yongli et al., 2015; Chang et al., 2013). The length of the amino–water hydrogen bond was shorter than those of the hydroxyl–water, amino–hydroxyl, and water–water hydrogen bonds. The bond angle was also smaller than those of the water–water and hydroxyl–water hydrogen bonds; this result indicated that the hydrogen bonds formed between the amino groups and water molecules were strong. The numbers of hydrogen bonds in the mixed systems changed with the changes in the mole ratios (Fig. 12(A)). Since the total number of water molecules remained constant for all systems, the numbers of hydrogen bonds within the water molecules themselves were consistent. Therefore, the three other interactions were responsible for the changes in the total number of hydrogen bonds. The amino groups with their three hydrogen atoms directly formed hydrogen bonds with at least three water molecules. The hydroxyl group had one hydrogen atom, and OCT was a nonionic surfactant; thus, it formed fewer hydrogen bonds with water molecules. Thus, the total number of hydrogen bonds was highest for the pure DDA system. Hydrogen bonding was one of the reasons for the high viscosity of the DDA flotation foam. The formation of many hydrogen bonds with high strengths slowed the drainage velocity of the liquid film and the gas diffusion velocity, prolonging the foam lifetime. With increasing OCT amount, the number of hydrogen bonds gradually decreased; thus, the stability and amount of the flotation foam gradually decreased.

Table 4. Bond angles and bond lengths for hydrogen bonds from different sources

Hydrogen bond	Hydrogen bond source			
	Amine–Hydroxyl	Amine–Water	Hydroxyl–Water	Water–Water
Hydrogen bond angle/°	147.31	151.37	151.56	152.86
Hydrogen bond length/Å	1.99	1.74	2.05	1.97

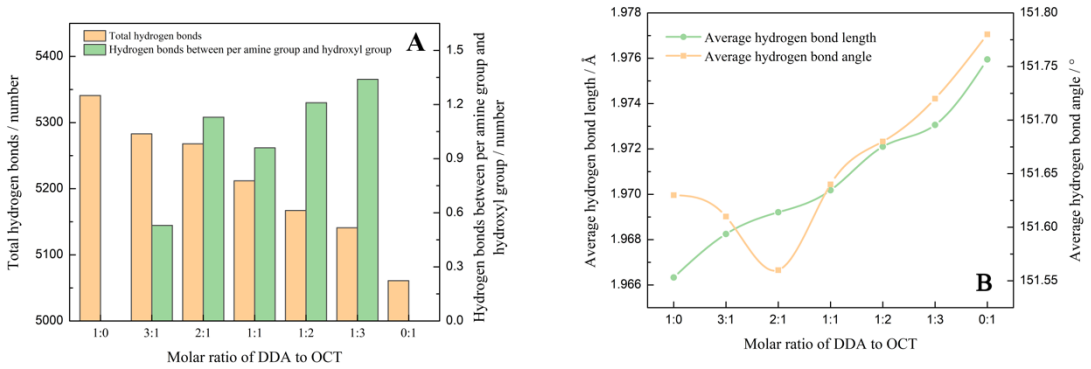

Fig. 12 Number (A), bond lengths and bond angles (B) of hydrogen bonds formed in the different systems.

With increasing OCT mole proportions, the average hydrogen bond lengths gradually increased, and the average hydrogen bond angles initially decreased and then increased; a minimum was reached at a mole ratio of 2:1 (Fig. 12 (B)). This phenomenon was ascribed to the greater number of hydrogen

bonds formed between the amino and hydroxyl groups (Fig. 12 (A) and Table 4). At this mole ratio, the energies of the hydrogen bonds were relatively high. Based on the above analyses, when the mole ratio was 2:1, the stability and amount of flotation foam significantly decreased due to reduction in the DDA amount. However, the changes in the lengths and bond angles of the hydrogen bonds caused a reduction in the sharp downward trend for the foam stability. Due to the reduced stability, the large volumes and high viscosities of the DDA flotation foams were overcome and the mineral desorption caused by foam rupture was improved. Additionally, the previously mentioned ion–dipole interactions and hydrophobic associations between DDA and OCT also played positive roles.

4. Conclusions

In this research, the flotation foam properties and self-aggregation behaviors of DDA/OCT mixtures with different mole ratios at the air/liquid interface were investigated by surface tension measurements, MD simulations and foam performance experiments. The MD simulation indicated that there was a synergistic effect between DDA and OCT during co-adsorption at the air/liquid interface. In the simulations, the DDA/OCT mixtures formed tightly packed monolayers with their head groups penetrating the water phase and their alkyl chains stretched into the air with different incline angles. Through hydrogen bonding and coulombic forces, OCT was inserted into the DDA adsorption layer, and the distance between the DDA cations increased, which reduced the electrostatic repulsions among amino groups and increased the adsorption capacities of the DDA/OCT mixtures at the air/liquid interface. The presence of OCT improved the hydration of the amino groups and increased the interfacial activities of the mixed surfactants. However, this improvement was closely related to the DDA/OCT mole ratio. With increases in the OCT mole proportion, the included angle formed between the alkyl chains of DDA and the interface showed an initial increase followed by a decrease, and the included angle reached a maximum at a DDA/OCT mole ratio of 2:1. The compatibilities of the alkyl chains also showed the same trend. At this mole ratio, there were relatively few hydrogen bonds in the mixed systems, and the hydrogen bond energy was relatively large. The presence of OCT improved the excessive stability of the DDA flotation foam caused by the electrostatic repulsions of the amino groups. Meanwhile, many hydrogen bonds with high strength were formed and the sharp downward trend for the foam stability with decreasing DDA amounts was reduced. Macroscopically, the stability of the DDA/OCT flotation foam was weaker than that of the pure DDA foam, and the high viscosity and difficult defoaming of the DDA flotation foam were significantly improved.

Acknowledgments

The financial support by the National Natural Science Foundation of China (Project No. 51674137) and the Natural Science Foundation of Shandong Province (Project No. ZR2022ME013) are sincerely appreciated.

References

BAHAREH, T., MAHDI, P., NASSER, S., MEHRDAD, H., MARI, K., MIKA, S., MIKA, M., 2014. *Removal of nickel ions from aqueous solution by micellar enhanced ultrafiltration, using mixed anionic–non-ionic surfactants*. Sep. Purif. Technol. 138, 169-176.

CHANG, Q., XI, Z., XIAOJIAN, F., WEITAO, Z., JER-LAI, K., YICHUN, Z., ZEXIANG, S., JI, Z., 2013. *Density and phonon-stiffness anomalies of water and ice in the full temperature range*. Journal of Physical Chemistry Letters. 4, 3238-3244.

FEI, M., JAMES, M., SHIRIN, S., AHMAD, G., 2021. *Review of lithium production and recovery from minerals, brines, and lithium-ion batteries*. Mineral Processing and Extractive Metallurgy Review. 42, 123-141.

GUPTA, A., BANERJEE, P., MISHRA, A., SATISH, P., PRADIP, 2007. Effect of alcohol and polyglycol ether frothers on foam stability, bubble size and coal flotation. International Journal of Mineral Processing. 82, 126-137.

HAO, J., WANYING, J., QINHONG, Y., LONGHUA, X., CHEN, Z., YUEHUA, H., 2017. *Synergistic adsorption and flotation of new mixed cationic/nonionic collectors on muscovite*. Minerals. 7, 74-85.

HAO, Z., CONG, H., WENGANG, L., DUANXU, H., DEZHOU, W., 2019. *The chain length and isomeric effects of monohydric alcohols on the flotation of magnesite and dolomite by sodium oleate*. Journal of Molecular Liquids. 276, 471-479.

HENDRIK, H., TZU, J., RATAN, K., FATEME, S., 2013. *Thermodynamically consistent force fields for the assembly of inorganic, organic, and biological nanostructures: the INTERFACE force field*. Langmuir. 29, 1754-1765.

JAEWOOK, L., HONGJIAN, Z., JAEBEOM, L., 2011. *Small molecule induced self-assembly of Au nanoparticles*. Journal of Materials Chemistry. 21, 16935-16942.

JESÚS A., MARCELA C., ANDRÉS M., JOSÉ M., FELIPE, J., 2019. *Blas Phase equilibria and interfacial properties of the tetrahydrofuran + methane binary mixture from experiment and computer simulation*. The Journal of Physical Chemistry C. 123, 1900-1906.

LASKOWSKI, J., CHO, Y., DING, K., 2003. *Effect of frothers on bubble size and foam stability in potash ore flotation systems*. The Canadian Journal of Chemical Engineering. 81, 63-69.

LIN T., HEINZ H., 2016. *Accurate force field parameters and pH resolved surface models for hydroxyapatite to understand structure, mechanics, hydration, and biological interfaces*. The, J. Phys. Chem. C. 120, 4975-4992.

LI, W., YUEHUA, H., JIAPENG, L., YONGSHENG, S., WEI, S., 2015. *Flotation and adsorption of muscovite using mixed cationic - nonionic surfactants as collector*. Powder technology. 276, 26-33.

LI, W., YUEHUA, H., RUNQING, L., JIAPENG, L., WEI, S., 2017. *Synergistic adsorption of DDA/alcohol mixtures at the air/water interface: A molecular dynamics simulation*. Journal of Molecular Liquids. 243, 1-8.

LI, W., RUNQING, L., YUEHUA, H., WEI, S., 2016. *Adsorption of mixed DDA/NaOL surfactants at the air/water interface by molecular dynamics simulations*. Chemical Engineering Science. 155, 167-174.

LONGHUA, X., YUEHUA, H., JIA, T., HOUQIN, W., LI, W., YAOHUI, Y., ZHEN, W., 2016. *Synergistic effect of mixed cationic/anionic collectors on flotation and adsorption of muscovite*. Colloids and Surfaces A: Physicochemical and Engineering Aspects. 492, 181-189.

LUCASSEN-REYNDERS, E., LUCASSEN, J., GILES, D., 1981. *Surface and bulk properties of mixed anionic/cationic surfactant systems i. equilibrium surface tensions*. J. Colloid Interface Sci. 81, 150-157.

MONTE, M., OLIVEIRA, J., 2004. *Flotation of sylvite with dodecylamine and the effect of added long chain alcohols*. Minerals Engineering. 17, 425-430.

NATHÁLIA V., FERNANDO O., CARLOS G., CARLOS A., MANUEL F., FERNANDA M., 2016. *Kinetic approach to the study of froth flotation applied to a lepidolite ore*. International Journal of Minerals, Metallurgy, and Materials, 23, 731-742.

NISHIKIDO, N., 1977. *Mixed micelles of polyoxyethylene - type nonionic and anionic surfactants in aqueous solutions*. J. Colloid Interface Sci. 60, 242-251.

PANKAJ, K., CHOUBEY, MIN-SEUK, K., RAJIV, R., SRIVASTAVA, JAE-CHUN L., JIN-YOUNG, L., 2016. *Advance review on the exploitation of the prominent energy - storage element: Lithium, Part I: From mineral and brine resources*. Minerals Engineering. 89, 119-137.

PUGH, R., RUTLAND, M., MANEV, E., CLAESSON P., 1996. *Dodecylamine collector - pH effect on mica flotation and correlation with thin aqueous foam film and surface force measurements*. Int. J. Miner. Process. 46, 245-262.

QINHONG Y., HAO J., WANYING J., JIAHUI X., YA G. YANG Q., JIANG H., JI W., 2018. *Mechanism of flotation of muscovite using mixed quaternary ammonium salt/octanol collectors*. The Chinese Journal of Nonferrous Metals. 28, 1900-1906.

SEKULIĆ, Ž., CANIĆ, N., BARTULOVIĆ, Z., DAKOVICC, A., 2004. *Application of different collectors in the flotation concentration of feldspar, mica and quartz sand.* Minerals Engineering. 17, 77-80.

SIMON, S., STEFAN, B., KAI, L., HANS, H., 2020. *Vapor-liquid interfacial properties of the system cyclohexane +CO_2: Experiments, molecular simulation and density gradient theory*. Fluid Phase Equilibria. 518, 112583-112597.

STEFAN, B., STEPHAN, W., MARTIN, H., KAI, L., HANS H., 2016. *Interfacial tension and adsorption in the binary system ethanol and carbon dioxide: Experiments, molecular simulation and density gradient theory.* Fluid Phase Equilibria. 427, 476-487.

SUFEN, Z., HAILIN, Z., XIN, L., ZHIYONG, H., DUANLIN, C., 2010. *Interaction of novel anionic Gemini surfactants with cetyltrimethylammonium bromide*. J. Colloid Interface Sci. 350, 480-485.

SZYMCZYK, K., JAŃCZUK, B., 2007. *The adsorption at solution–air interface and volumetric properties of mixtures of cationic and nonionic surfactants*. Colloids Surf. A Physicochem. Eng. Asp. 293, 39-50.

TAOTAO, Z., GUIYING, X., SHILING, Y., YIJIAN, C., HUI, Y., 2010. *Molecular dynamics study of alkyl benzene sulfonate at air/water interface: effect of inorganic salts*. J. Phys. Chem. B. 114, 5025-5033.

VIDYADHAR, A., KUMARI, N., BHAGAT, R., 2012. *Adsorption mechanism of mixed collector systems on hematite flotation*, Miner. Eng. 26, 102-104.

WENFENG, L., HAINAN, W., XIN, L., YANNAN, L., YONGTIAN, W., HAIJUN, Z., 2021. *Effect of mixed cationic/anionic surfactants on the low-rank coal wettability by an experimental and molecular dynamics simulation*. Fuel. 289, 119886-119895.

XIMEI, L., LINPING, Q., SHUMING, W., YUNFAN, W., HAO, L., QIQIANG, L., YONGFENG, Z., XUETONG, W., ZHENGUO, S., 2021. *Adsorption configuration of dodecylamine at gas–liquid interface and its relationship with foam stability: MD simulation and ToF-SIMS investigation*. Minerals Engineering, 164, 106830-106844.

YANG B., WANSHUN C., YUJUAN G., WEIXIANG W., YIKUN S., PINGKE YA., 2023. *Synergistic mechanism of mixed cationic/anionic collectors on lepidolite flotation from the perspective of improving the performance of flotation foam*. Colloids and Surfaces A: Physicochemical and Engineering Aspects. 656, 130354-130364.

YANG, B., WEIXIANG, W., YUJUAN, G., WANSHUN, C., YIKUN, S., PINGKE, Y., 2022. *Molecular dynamics simulations of the structure - property relationships of DDA/anionic surfactant mixtures at the air/water interface*. Journal of Molecular Liquids. 368, 120804-120815.

YANG, Z., JINCHENG, M., JINZHOU, Z., ZHENGJIE, L., TAO, X., JINHUA, M., HAILIN, S., LIJUN, Z., YONGHAO, N., 2021. *Synergy between different sulfobetaine-type zwitterionic Gemini surfactants: Surface tension and rheological properties*. Journal of Molecular Liquids. 332, 115141-115150.

YONGLI, H., XI, ZHANG., ZENGSHENG, M., YICHUN, Z., WEITAO, Z., JI, Z., CHANG, Q., 2015. *Hydrogen-bond relaxation dynamics: resolving mysteries of water ice*. Coordination Chemistry Reviews. 285, 109-165.

ZHIQIANG, H., SHUYI, S., HONGLING, W., RUKUAN, L., SHIYONG, Z., CHEN, G., YAJING, H., XINYANG, Y., GUICHUN, H., WENG, F., 2021. *Froth flotation separation of lepidolite ore using a new Gemini surfactant as the flotation collector*. Separation and Purification Technology. 282, 119122-119147.